Exploring the ultra-high-precision ranging potential of BDS B1 signal

Yang Gao[1,2,3], Zheng Yao[1,2], Mingquan Lu[1,2]

1. *Department of Electronic Engineering, Tsinghua University, Beijing, China*
2. *Beijing National Research Center for Information Science and Technology, Beijing, China*
3. *Beijing Satellite Navigation Center, Beijing, China*

BIOGRAPHIES

Yang Gao is currently a Ph.D. candidate in information and communication engineering at the Department of Electronic Engineering in Tsinghua University, Beijing, China. He received the B.Eng. degree in electronic information science and technology in 2013 from Tsinghua University. His current research focuses on new generation GNSS signal processing and real-time GNSS software receiver.

Zheng Yao is an Associate Professor with the Department of Electronic Engineering, Tsinghua University, Beijing, China. He received the B.S. degree in Electronics Information Engineering and the Ph.D. degrees (with the highest honors) in Information and Communication Engineering from Tsinghua University, Beijing, China, in 2005 and 2010, respectively. His current research mainly targets next-generation satellite navigation signals design, software-defined receiver, new location technologies, and personal and vehicular positioning in challenging environments.

Mingquan Lu is a Professor with the Department of Electronic Engineering, Tsinghua University, Beijing, China. He received the M.E. and Ph.D. degrees in Electrical Engineering from the University of Electronic Science and Technology of China, Chengdu, China. He directs the Positioning, Navigation and Timing (PNT) Research Center, which develops GNSS and other PNT technologies. His current research interests include GNSS system modeling and simulation, signal design and processing.

ABSTRACT

In BDS-3 B1 band, a unique single-sideband complex binary offset carrier (SCBOC) modulation type was introduced as a multi-frequency multiplexing technique to achieve the backward compatibility with the traditional B1I BPSK(2) modulated signal. However, the SCBOC should have the ability to participate in the pseudorange measurement like other BOC-class subcarriers instead of just being regarded as a transparent multiplexing tool. In addition, since the SCBOC(14,2) modulated signal has a high-frequency subcarrier, it may contain the ultra-high-performance ranging potential, which is very valuable and worthy of attention. Therefore, this paper first analyses the ranging potential and tracking challenges of the SCBOC(14,2) modulated signal, and then proposes an example solution to explore the ultra-high-precision ranging potential of the BDS-3 B1 signal. Real experimental results using live BDS-3 signals verified the correctness and effectiveness of the proposed algorithm. For BDS receiver designers who are interested in the high-precision ranging, this paper can provide great guidance and reference.

1. INTRODUCTION

33rd International Technical Meeting of the Satellite Division of the Institute of Navigation (ION GNSS+ 2020), September 22-25, 2020

3626

https://doi.org/10.33012/2020.17678

In recent years, the Beidou navigation satellite system (BDS) has entered its third construction stage, which is referred to as BDS-3 and is upgrading from a regional system to a global system. In order to achieve the backward compatibility, the traditional B1I signal is still broadcast by BDS-3 satellites in B1 band. Besides, the new civil signal B1C and authorized service signal B1A are also added in BDS-3 B1 band. In order to save the resource cost of the satellite payload and expand the service life of the navigation satellite, the signals in the same band should share the same transmitting link as much as possible. Therefore, these three useful signals should first combine into a baseband composite signal, and then are broadcast through the shared carrier. However, the center frequency of the traditional B1I signal and that of the new B1C/B1A signal are different. In addition, the constant-envelope constraint still exists for the BDS-3 B1 composite signal. Therefore, new modulation and multiplexing technologies need to be applied in BDS-3 B1 band to meet these demands and constraints. More specifically, the SCBOC(14,2) modulation [1] is applied in the B1I signal to shift the center frequency from 1575.42 MHz to 1561.098 MHz. Besides, the versatile and exquisite constant envelope multiplexing via intermodulation construction (CEMIC) technique [2, 3] is adopted in the B1 band to achieve the wideband constant-envelope composite navigation signal.

For a long time in the past, since the SCBOC(14,2) modulated signal adopts a single complex subcarrier and has an asymmetrical spectrum, which is different from other existing binary phase shift keying (BPSK) and BOC-class modulated signals in GNSS community, the SCBOC is just regarded as a transparent multiplexing component to achieve the backward compatibility. However, these understandings are insufficient and biased. First, the SCBOC is able to participate in the pseudorange measurement like other BOC-class subcarriers instead of just being regarded as a transparent multiplexing tool. Second, since the SCBOC(14,2) modulated signal has a high-frequency subcarrier, it may contain the ultra-high-performance ranging potential. Therefore, if the SCBOC(14,2) modulated signal is just treated as a traditional BPSK(2) modulated signal, the ultra-high-precision ranging potential it contains will be greatly wasted. So exploring the effective use of this great ranging potential is very valuable and worthy of attention.

Before utilizing the ranging potential, there are two main tracking challenges need to be solved. First, the auto-correlation function (ACF) of the SCBOC (14,2) modulated signal has multiple side peaks, which means that it is possible to track the side peaks instead of the main peak. This is the well-known tracking ambiguity threat in BOC-class modulated signals. Considering that the modulation order of the SCBOC(14,2) modulated signal is large, its tracking ambiguity threat is great. Second, the ACF of the SCBOC(14,2) modulated signal is a complex function, whose imaginary part is not constant. This feature is different from the existing BPSK and BOC-class modulated signals. Since the carrier will appear in both real and imaginary parts, such a complex correlation peak generally cannot be tracked by traditional receivers [4]. More specifically, when the subcarrier phase of the local replica is not aligned with that of the received signal, the energy moves from the real part to the imaginary part, which will cause the estimation deviation of the carrier phase, and vice versa. These tracking challenges prevent the exploring the ranging potential of the SCBOC(14,2) modulated signal.

For the tracking ambiguity threat, the two-dimensional (2-D) loop structures [5-9], which solve the ambiguity problem by adding an additional subcarrier loop to independently track the subcarrier dimensional phase delay and transform the signal correlation function into a two-dimensional space, are verified [10-12] to be more general and suitable for high-order BOC modulated signals like SCBOC(14,2) modulated signal than other unambiguous tracking methods. However, all of the existing 2-D solutions can only be used for signals whose ACFs are real functions, thus cannot be directly used for SCBOC(14,2) modulated signal. As for the tracking instability of the complex correlation function, there are few solutions existing in the GNSS community. The only one possible solution is the traditional BPSK-Like technique [13], which treats the subcarrier as part of the carrier. However, such an unmatched reception mode pays a great price in ranging performance because the whole ranging ability of high-frequency subcarrier is lost. These challenges hinder the understanding and utilization of SCBOC modulated signals.

To solve these problems and challenges, an unambiguous tracking method is proposed to be an example solution to explore the ultra-high-precision ranging potential of the BDS B1 signal. More detailed, it uses a 2-dimensional loop structure to address the ambiguity threat inherent in BOC-class modulated signals. In addition, based on the coherence between the components of

the composite signal, the proposed method uses cross-assisted technique to solve the coupling problem in the correlation function between subcarrier and carrier while improving the receiver robustness. Real experimental results using live BDS-3 signals verified the correctness and effectiveness of the proposed algorithm. For BDS receiver designers who are interested in the high-precision ranging, this paper can provide great guidance and reference.
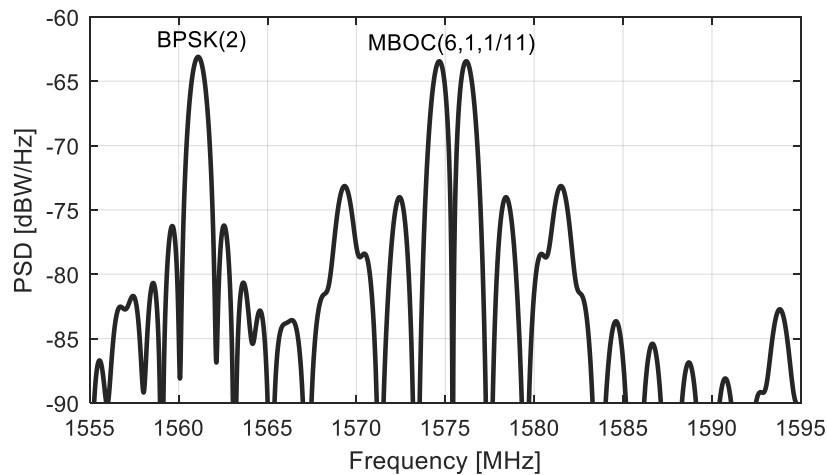
The remainder of the paper is organized as follows. Section 2 describes the model and characteristics of the BDS-3 B1 wideband composite signal. Then, the proposed tracking method is presented in Section 3. Next, the real experimental results are provided in Section 4. Finally, conclusions and future work are discussed in Section 5.

2. SIGNAL MODEL AND CHARACTERISTICS

This section will first introduce the generation background and signal model of the BDS-3 B1 wideband composite signal. Then the spectrum characteristics of the new SCBOC(14,2) modulated signal are analyzed. Finally, the ranging potential and tracking challenges of the BDS-3 B1I signal are also given.

Background

Figure 1 shows the spectrum constraints of the BDS-3 B1 band. Note that only civil signals are considered here. As can be seen from Figure 1, the traditional B1I signal, whose modulation type is BPSK(2), and central frequency is located at 1561.098 MHz, still needs to be broadcast by the BDS-3 satellites for the backward compatibility. In addition, for the compatible interoperability with GPS L1C signal and Galileo E1 signal, the new B1C signal needs to be broadcast at 1575.42 MHz and meet the MBOC(6,1,1/11) spectrum constraint [14, 15]. Besides, with the increasing demand of advanced users for navigation and positioning, a new authorized service signal B1A also needs to be broadcast at 1575.42 MHz by BDS-3 satellites. Therefore, there are three useful signals simultaneously in BDS-3 B1 band, which are the B1I signal for backward compatibility, the B1C signal for compatible interoperability, and the B1A signal for authorized services.
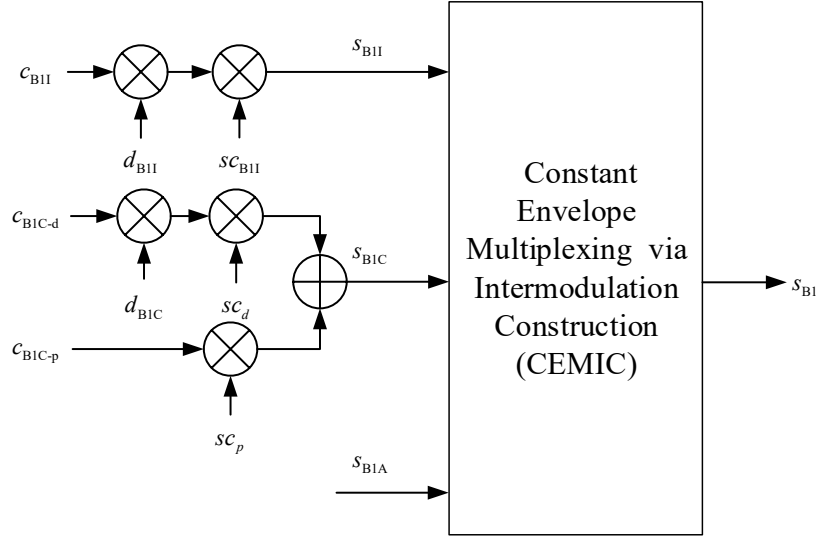

Figure 1: The spectrum constraints of the BDS-3 B1 band (civil signals only)

As we all know, the navigation signals in the same band should share the transmitting link as much as possible to save the resources cost of the satellite payload and expand the life length of the navigation satellite. Therefore, these three useful signals in the B1 band need to combine into a wideband composite signal and then be broadcast by BDS-3 satellites. However, the center frequency of the traditional B1I signal and that of the new B1C/B1A signals are different. In addition, the constant-envelope constraint still exists for the BDS-3 B1 composite signal. Therefore, new modulation and multiplexing technologies need to be developed to meet these demands and constraints.

Signal Model

In order to meet these demands and constraints, new modulation and multiplexing techniques are developed and applied in the BDS-3 B1 band. More specifically, the QMBOC(6,1,1/11) modulation [16] is used in the B1C signal to meet the spectrum constraint. Besides, the SCBOC(14,2) modulation is applied in the B1I signal to shift the center frequency from 1575.42 MHz to 1561.098 MHz. Finally, the versatile and exquisite CEMIC technique is adopted in the B1 band to achieve the wideband constant-envelope composite navigation signal.

Figure 2 shows the generation scheme of the BDS-3 B1 wideband composite signal. Note that only the generation of baseband composite signal is given here. In addition, only useful signals are represented in Figure 2.

Figure 2: The generation scheme of the BDS-3 B1 wideband composite signal

Therefore, the BDS-3 B1 wideband radio frequency (RF) composite signal can be modeled as:

$$S_{\mathrm{B1}}(t) = \mathrm{Re}\left\{\left(\sqrt{P_{\mathrm{B1I}}}\,\mathrm{e}^{\mathrm{j}\phi_{\mathrm{B1I}}}s_{\mathrm{B1I}}(t) + \sqrt{P_{\mathrm{B1C}}}\,\mathrm{e}^{\mathrm{j}\phi_{\mathrm{B1C}}}s_{\mathrm{B1C}}(t) + \sqrt{P_{\mathrm{B1A}}}\,\mathrm{e}^{\mathrm{j}\phi_{\mathrm{B1A}}}s_{\mathrm{B1A}}(t) + I_{\mathrm{IM}}(t)\right)\mathrm{e}^{\mathrm{j}2\pi f_{\mathrm{B1}}t}\right\} \quad (1)$$

where P_i, ϕ_i, and $s_i(t)$ are the nominal power, initial phase, and baseband complex envelope of the corresponding signal component $i = \mathrm{B1I, B1C, B1A}$, respectively. The initial phases ϕ_{B1I} and ϕ_{B1C} are equal, and the baseband complex envelope can be further given by

$$s_{\mathrm{B1I}}(t) = c_{\mathrm{B1I}}(t)d_{\mathrm{B1I}}(t)sc_{\mathrm{B1I}}(t) \quad (2)$$

$$s_{\mathrm{B1C}}(t) = \frac{1}{2}d_{\mathrm{B1C}}(t)c_{\mathrm{B1C-d}}(t)sc_d(t) + c_{\mathrm{B1C-p}}(t)\left[\underbrace{\sqrt{\frac{1}{11}}sc_b(t) + \mathrm{j}\cdot\sqrt{\frac{29}{44}}sc_d(t)}_{sc_p(t)}\right] \quad (3)$$

where $d_{\mathrm{B1I}}(t)$ and $d_{\mathrm{B1C}}(t)$ are the navigation messages of B1I and B1C signal, respectively. $c_{\mathrm{B1I}}(t)$, $c_{\mathrm{B1C-d}}(t)$, and $c_{\mathrm{B1C-p}}(t)$ are the ranging codes of the B1I signal, data channel, and pilot channel of B1C signal, respectively. $sc_d(t) = \mathrm{sgn}\left(\sin\left(2\pi f_{sc,a}t\right)\right)$ and $sc_b(t) = \mathrm{sgn}\left(\sin\left(2\pi f_{sc,b}t\right)\right)$ are the sine-phased square wave subcarriers with subcarrier

frequency $f_{sc,a} = 1f_0$ and $f_{sc,b} = 6f_0$ used by the narrowband BOC(1,1) component and the wideband BOC(6,1) component, respectively, where $f_0 = 1.023$ MHz is the GNSS baseline frequency.

$$sc_{B1I}(t) = \text{sgn}\left(\cos\left(2\pi f_{sc,B1I}t\right)\right) - j \cdot \text{sgn}\left(\sin\left(2\pi f_{sc,B1I}t\right)\right) \qquad (4)$$

is the single-sideband complex subcarrier with the frequency of $f_{sc,B1I} = 14f_0$, where $\text{sgn}(x)$ is the sign function which takes value of 1 for $x \geq 0$ and -1 for $x < 0$. $I_{IM}(t)$ is the additional intermodulation term to maintain the constant envelope of the composite signal.

Ignoring the authorized signal B1A, the received B1 wideband composite signal (open part) at the antenna of the GNSS receiver can be represented as

$$
\begin{aligned}
r_{B1}(t) = &\underbrace{\sqrt{P_{B1I}}\, d_{B1I}(t-\tau)\, c_{B1I}(t-\tau)\left[\begin{array}{l}\text{sgn}\left(\cos\left(2\pi f_{sc,B1I}(t-\tau)\right)\right)\cos\left(2\pi\left(f_{B1}+f_D\right)t+\varphi\right) \\ +\text{sgn}\left(\sin\left(2\pi f_{sc,B1I}(t-\tau)\right)\right)\sin\left(2\pi\left(f_{B1}+f_D\right)t+\varphi\right)\end{array}\right]}_{r_{B1I}(t)} \\
&+\underbrace{\frac{1}{2}\sqrt{P_{B1C}}\, d_{B1C}(t-\tau)\, c_{B1C-d}(t-\tau)\, sc_a(t-\tau)\cos\left(2\pi\left(f_{B1}+f_D\right)t+\varphi\right)}_{r_{B1C-d}(t)} \\
&+\underbrace{\sqrt{\frac{P_{B1C}}{11}}\, c_{B1C-p}(t-\tau)\, sc_b(t-\tau)\cos\left(2\pi\left(f_{B1}+f_D\right)t+\varphi\right)}_{r_{B1C-pb}(t)} \\
&-\underbrace{\sqrt{\frac{29P_{B1C}}{44}}\, c_{B1C-p}(t-\tau)\, sc_a(t-\tau)\sin\left(2\pi\left(f_{B1}+f_D\right)t+\varphi\right)}_{r_{B1C-pa}(t)} \\
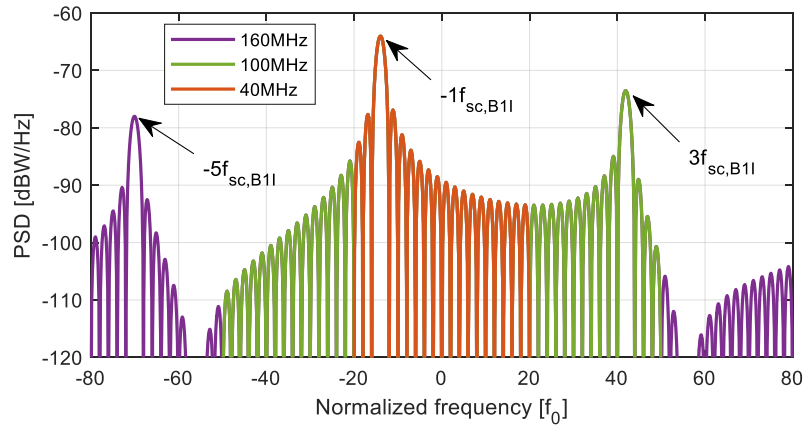&+n(t)
\end{aligned}
\qquad (5)
$$

where τ is the signal propagation delay, f_{B1} is the center frequency, f_D is the Doppler shift, φ is the carrier phase, $n(t)$ is the zero-mean Gaussian white noise with PSD N_0.

Spectrum Characteristics

In order to have a better understanding about the new SCBOC(14,2) modulated signal and B1 wideband composite signal, their spectrum characteristics are given below and analyzed in detail.
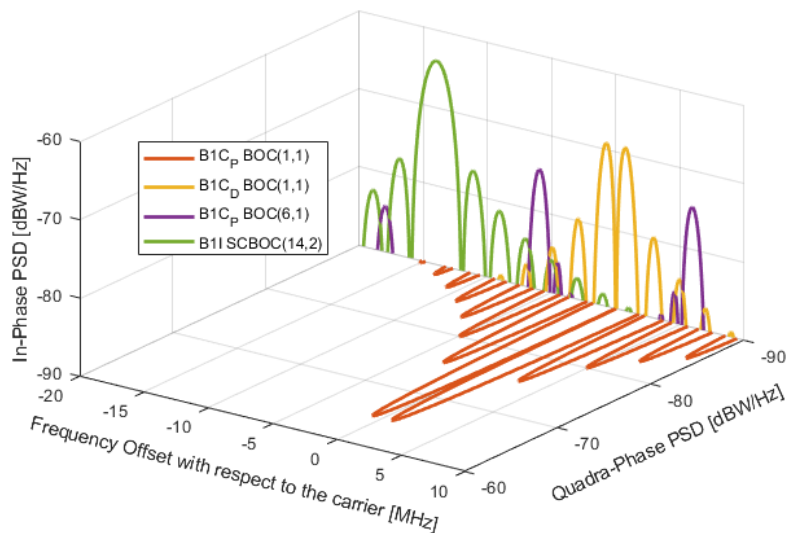
Figure 3 shows the power spectral density (PSD) of the SCBOC(14,2) modulated signal with different filter bandwidths. First, it can be seen from Figure 3 that the first main lobe of the SCBOC(14,2) modulated signal is shifted from the center frequency to the lower sideband, which maintains the backward compatibility with the traditional B1I signal. Second, the PSD of the SCBOC(14,2) modulated signal is asymmetric about the central frequency, which is different from BPSK and other BOC-class modulated signals. This is because the main harmonic component of the single-sideband complex subcarrier is only concentrated at $-f_{sc,B1I}$ while no harmonic component exists at $f_{sc,B1I}$. Third, it is not difficult to find that in order to contain the second side lobe of the SCBOC(14,2) modulated signal, the filter bandwidth should be at least 90.024 MHz, which is too wide for the existing receiver front-end. Therefore, for a general receiver, whose front-end bandwidth is in the range of 32.736 MHz to 90.024 MHz, all the high-frequency components of the square-wave subcarrier will be removed, and only the first-order term will be

preserved, which means the square subcarrier should be approximated as pure sinusoid wave, that is $sc_{B1I}(t) \approx \cos(2\pi f_{sc,B1I}t) - \mathrm{j} \cdot \sin(2\pi f_{sc,B1I}t)$. Note that the real experimental results using live BDS-3 signals in section 4 also show that this subcarrier approximation is reasonable. Substituting this approximation into Equation (5) to obtain the final signal model.

Figure 3: The power spectral density of the SCBOC(14,2) modulated signal with different filter bandwidths

Figure 4 shows the spectrum of the BDS-3 B1 wideband composite signal in (5). Note that only the civil signals are considered here. It can be seen from Figure 4 that the spectrums of the B1I SCBOC(14,2) modulated signal, the BOC(1,1) component of B1C data channel, and the BOC(6,1) component of B1C pilot channel are in the in-phase branch, while the spectrum of the BOC(1,1) component of B1C pilot channel is in the quadrature branch. Considering that the pilot channel will not be influenced by the navigation bits and the BOC(1,1) component takes up the most of the power of the pilot channel, only the pilot BOC(1,1) component is considered for the B1C signal in (5) in the following sections.

Figure 4: The spectrum of the BDS-3 B1 wideband composite signal (civil signals only)
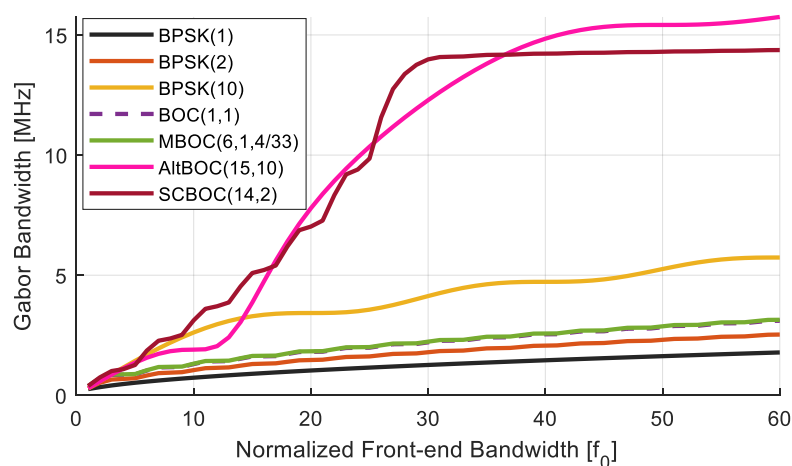
Comparing the Figure 1 and Figure 4, the BDS-3 SCBOC(14,2) modulated signal can achieve the backward compatibility with the traditional B1I BPSK(2) modulated signal. For a long time in the past, considering that the SCBOC(14,2) modulated signal adopts a single complex subcarrier and has an asymmetrical spectrum, which is different from other existing BSPK and

BOC-class modulated signals in GNSS community, the SCBOC is just regarded as a transparent multiplexing component before this paper. However, these understandings are insufficient and biased. First, the SCBOC is able to participate in the pseudorange measurement similar to other BOC-class subcarriers, not just a transparent multiplexing component. Second, since the higher the subcarrier frequency, the higher the ranging precision, therefore, the SCBOC(14,2) modulated signal may contain the ultra-high-performance ranging potential. Third, since the single complex subcarrier is introduced in the SCBOC(14,2) modulated signal, some new complicated tracking challenges may occur. However, with new ideas and signal structures, these difficulties can be solved. Therefore, the following will focus on the ranging potential and tracking challenges of the SCBOC(14,2) modulated signal.

Ranging Potential

In GNSS community, the Gabor bandwidth, which is determined by the PSD of the navigation signal, is always used as a quantitative indicator to describe the signal ranging potential. The greater the Gabor bandwidth is, the higher the ranging potential is. Note that the Gabor bandwidth belongs to the signal characteristics and has nothing to do with the specific tracking method.

Figure 5 shows the comparison of all civil signals in GNSS community in terms of the Gabor bandwidth. As can be seen from Figure 5, all civil signals can be divided into three levels according to the Gabor bandwidth. The most advanced level has the largest Gabor bandwidth, which means these signals have the greatest ranging potential, including AltBOC(15,10) [17] and SCBOC(14,2) modulated signals. The medium level has the intermediate Gabor bandwidth and good ranging potential, including BPSK(10) modulated signal. The lowest level has the minimum Gabor bandwidth and the worst ranging potential, including BSPK(1), BPSK(2), BOC(1,1), and MBOC(6,1,4/33) modulated signals. Therefore, the SCBOC(14,2) modulated signal has the first-class Gabor bandwidth, and if only it is received as a traditional BPSK(2) modulated signal, the ultra-high-precision ranging potential it contains will be greatly wasted. So exploring the effective use of this great ranging potential in the SCBOC(14,2) modulated signal is very valuable and worthy of attention.
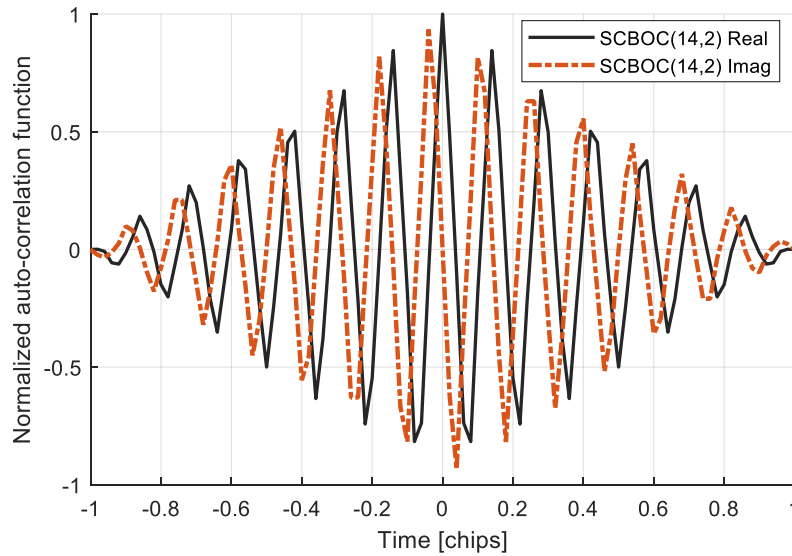

Figure 5: The comparison of all civil signals in GNSS community in terms of the Gabor bandwidth

Tracking Challenges

Before introducing the methodology, a full understanding of the tracking challenges is required. Therefore, the ACF is used here to help understand the difficulties and challenges qualitatively when tracking the SCBOC(14,2) modulated signals.

Figure 6 shows the ideal ACF of the SCBOC(14,2) modulated signal. It can be seen from Figure 6 that there are two main tracking challenges. First, the ACF of the SCBOC (14,2) modulated signal has multiple side peaks, which means that it is possible

to track the side peaks instead of the main peak. This is the well-known tracking ambiguity threat in BOC-class modulated signals. Considering that the modulation order of the SCBOC(14,2) modulated signal is large, its tracking ambiguity threat is great. Second, the ACF of the SCBOC(14,2) modulated signal is a complex function, whose imaginary part is not constant. This feature is different from the existing BPSK and BOC-class modulated signals. Since the carrier will appear in both real and imaginary parts, such a complex correlation peak generally cannot be tracked by traditional receivers. More specifically, when the subcarrier phase of the local replica is not aligned with that of the received signal, the energy moves from the real part to the imaginary part, which will cause the estimation deviation of the carrier phase, and vice versa. These tracking challenges prevent the exploring the ranging potential of the SCBOC(14,2) modulated signal.

Figure 6: The ideal auto-correlation function of the SCBOC(14,2) modulated signal
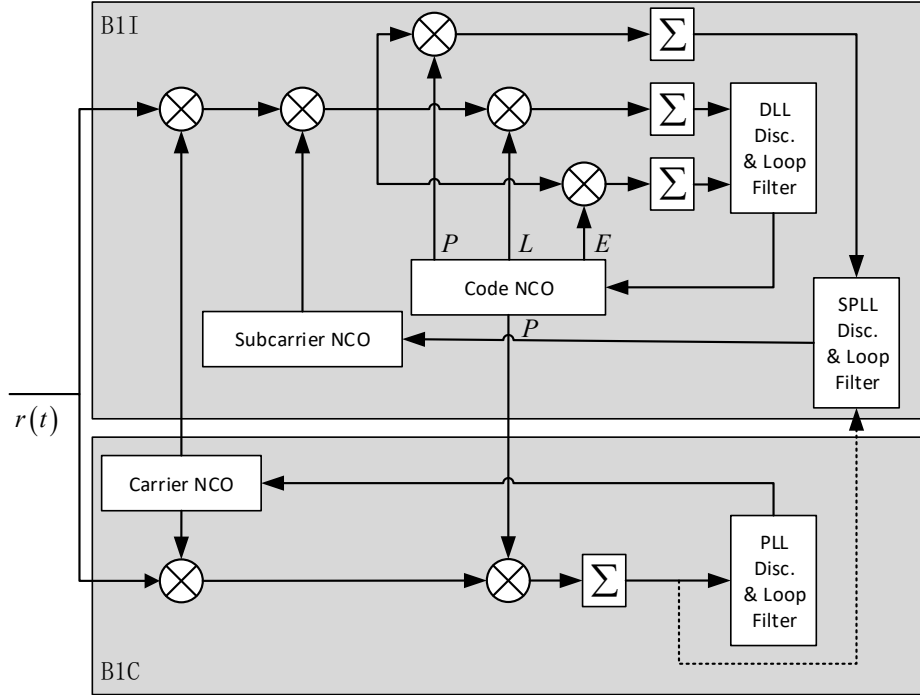
3. METHODOLOGY

The previous section analyzed the ranging potential and tracking challenges of the BDS-3 SCBOC(14,2) modulated signal from a theoretical point of view. This section will give a possible solution to overcome these tracking challenges and exploit this ranging potential. The proposed method can be an example to provide reference and reference for receiver designers, who are interested in the high-precision ranging of the BDS-3 signals.

Figure 7 shows the schematic representation of the proposed tracking method for BDS-3 B1 wideband composite signal. Different from the traditional receiver, it can be seen from Figure 7 that there are three main differences. First, since the SCBOC(14,2) modulated signal cannot be tracked alone in matched reception mode, the B1C signal is introduced to work at the same time. More specifically, since the SCBOC(14,2) modulated signal and the B1C signal share the same carrier, the carrier estimate of the composite signal can be obtained by the B1C component, which doesn't have the complex coupling relationship between the carrier and subcarrier like the B1I signal. Therefore, when the carrier of the SCBOC(14,2) modulated signal can be perfectly recovered from that of the B1C component, the coupling relation between the estimation errors of subcarrier and carrier can be effectively separated, which means the complex subcarrier can also be tracked alone and the receiver works in the matched reception mode. Second, a 2-D tracking loop architecture is used in the tracking phase of the SCBOC(14,2) modulated signal to transform the signal correlation function into a 2-D space to solve the serious tracking ambiguity threat. More specifically, an unambiguous but low-precision phase delay estimation in the code dimension can be tracked by a conventional delay lock loop (DLL), and a high-precision but ambiguous phase delay estimation in the subcarrier dimension can be obtained by an additional

subcarrier phase lock loop (SPLL). Then the two phase delay estimations can be recombined to develop the final unambiguous and high-precision propagation delay estimation. Third, the locally replicated B1I and B1C signal use the same code NCO to recover the propagation delay estimation of the composite signal. More detailed, only the prompt propagation delay of the B1C code and subcarrier needs to be recovered by that of the B1I component, which will eliminate the ambiguity threat of the B1C signal and improve the receiver robustness. For more details and extensions of this algorithm, the reader can refer to our research [18].

Figure 7: The schematic representation of the proposed tracking method for BDS-3 B1 composite signal

At first, the carrier of the B1C pilot BOC(1,1) component and B1I signal can be removed from the received B1 composite

signal $r_{B1}(t)$ by multiplying locally replicated complex carrier $y_{B1C}(t) = e^{-j\left(2\pi\left(f_{B1}+\hat{f}_D\right)t+\hat{\varphi}+\pi/2\right)}$ and $y_{B1I}(t) = e^{-j\left(2\pi\left(f_{B1}+\hat{f}_D\right)t+\hat{\varphi}\right)}$,

where $\hat{f}_D$ and $\hat{\varphi}$ are the estimations of Doppler shift and carrier phase, respectively. Then, the complex subcarrier of the

SCBOC(14,2) modulated signal can be removed by multiplying the complex conjugate of the subcarrier exponential, that is

$sc_{B1I}^*(t) = e^{j\left(2\pi\hat{f}_{sc,B1I}t-\hat{\varphi}_{sc,B1I}\right)}$, where $\hat{f}_{sc,B1I}$ is the estimation of the subcarrier frequency, $\hat{\varphi}_{sc,B1I} = 2\pi\hat{f}_{sc,B1I}\hat{\tau}_s$ is the estimation of

the subcarrier phase, and $\hat{\tau}_s$ is the phase delay estimation in the subcarrier dimension.

Next, the product of the locally generated code with the received signal is subjected to the coherent integration to calculate the correlators output results

$$R_{i\text{-B1I}} = \frac{1}{T}\int_0^T r_{B1}(t) \cdot y_{B1I}(t) \cdot sc_{B1I}^*(t) \cdot c_{B1I}\left(t-\hat{\tau}_c+\tau_i'\right) \cdot dt$$

$$R_{\text{P-B1C}} = \frac{1}{T}\int_0^T r_{B1}(t) \cdot y_{B1C}(t) c_{B1C\text{-p}}\left(t-\hat{\tau}_c\right) \cdot \text{sgn}\left(\sin\left(2\pi f_{sc,a}\left(t-\hat{\tau}_c\right)\right)\right) \cdot dt$$

(6)

where T is the coherent integration time, $\hat{\tau}_c$ is the phase delay estimation in code dimension, the subscript $i \in \{\text{E,P,L}\}$

stands for the branches of early (E), prompt (P), and late (L) correlator outputs, with the additional phase delays of $\tau_E' = -\Delta_c/2$,

$\tau_P' = 0$, and $\tau_L' = \Delta_c/2$, respectively, in which Δ_c is the spacing between E and L replicas for the code discriminator and it

is assumed to be in the range $0 \le \Delta_c \le T_c$. Note that only P correlator is needed for the tracking of the B1C signal.

Therefore, the corresponding correlators output can be expressed as

$$R_{i-\text{B1I}} = d\sqrt{2P_{B1I}}\Lambda_{B1I}\left(\tau - \hat{\tau}_c + \tau'\right)\text{sinc}\left(\left(\Delta f_D - \Delta f_{sc,B1I}\right)T\right)e^{j\left(\pi\left(\Delta f_D - \Delta f_{sc,B1I}\right)T + \Delta\varphi + \Delta\varphi_{sc,B1I}\right)}$$
$$R_{\text{P-B1C}} = \sqrt{2P_{B1C}}W_{B1C}\left(\tau - \hat{\tau}_c\right)\text{sinc}\left(\Delta f_D T\right)e^{j\left(\pi\Delta f_D T + \Delta\varphi\right)} \tag{7}$$

where $\Lambda_{B1I}\left(\tau - \hat{\tau}_c\right)$ is the code dimension ACF of the SCBOC(14,2) modulated signal, $W_{B1C}\left(\tau - \hat{\tau}_c\right)$ is the ACF of the B1C

pilot BOC(1,1) component, $\Delta f_D = f_D - \hat{f}_D$ and $\Delta\varphi = \varphi - \hat{\varphi}$ are the corresponding estimation errors, respectively.

$\Delta f_{sc,B1I} = f_{sc,B1I} - \hat{f}_{sc,B1I}$ is the subcarrier frequency estimation error, and $\Delta\varphi_{sc,B1I} \triangleq 2\pi\left(f_{sc,B1I}\tau - \hat{f}_{sc,B1I}\hat{\tau}_s\right)$ is the subcarrier

phase estimation error.

By assuming the perfect Doppler shift and subcarrier frequency synchronization, that is, $\Delta f_D \approx 0$ and $\Delta f_{sc,B1I} \approx 0$, the

correlators outputs (7) can be further simplified as

$$R_{i-\text{B1I}} = d\sqrt{2P_{B1I}}\Lambda_{B1I}\left(\tau - \hat{\tau}_c + \tau'\right)e^{j\left(\Delta\varphi + \Delta\varphi_{sc,B1I}\right)}$$
$$R_{\text{P-B1C}} = \sqrt{2P_{B1C}}W_{B1C}\left(\tau - \hat{\tau}_c\right)e^{j\Delta\varphi} \tag{8}$$

Then, $R_{\text{E-B1I}}$ and $R_{\text{L-B1I}}$ are input to the standard DLL discriminators to get the code phase estimation error. Meanwhile, $R_{\text{P-B1C}}$ is input to the standard PLL discriminators to obtain the carrier phase estimation error $\Delta\varphi$. Considering the DLL and PLL used here are the standard loop structure, detailed operations are not discussed further.

As for the additional SPLL, two classes of discriminators can be employed, which are the coherent discriminators neglecting the residual carrier phase error ($\Delta\varphi = 0$) and non-coherent discriminators in the presence of the residual carrier phase errors ($\Delta\varphi \ne 0$). For the coherent discriminators, an example can be

$$\phi_{c,SCBOC}\left(\Delta\varphi_{sc,B1I}\right) = \arctan\left(\frac{\text{Re}\left(R_{\text{P-B1I}}\right)}{\text{Im}\left(R_{\text{P-B1I}}\right)}\right) \tag{9}$$

when the residual carrier phase is small enough and can be approximated as $\Delta\varphi = 0$, the $R_{\text{P-B1I}}$ correlator results can be directly used to calculate the subcarrier phase estimation error. For the non-coherent discriminators, an example can be

$$\phi_{nc,SCBOC}\left(\Delta\varphi_{sc,B1I}\right) = \arctan\left(\frac{\text{Re}\left(R_{\text{P-B1I}}R_{\text{P-B1C}}^*\right)}{\text{Im}\left(R_{\text{P-B1I}}R_{\text{P-B1C}}^*\right)}\right) \tag{10}$$

where $*$ represents conjugate operator. The working principle of (10) can be easily verified by trigonometric identity. Finally, the filtered subcarrier phase estimation is input to the subcarrier NCO to update the locally generated complex subcarrier $sc_{B1I}^*(t)$, thus closing the tracking loop.

When the unambiguous but low-precision code dimension delay estimation $\hat{\tau}_c$ and the high-precision but ambiguous subcarrier dimension delay estimation $\hat{\tau}_s$ are obtained, the final ultra-high-precision propagation delay estimation $\hat{\tau}$ can be represented as

$$\hat{\tau} = \hat{\tau}_s + \text{round}\left(\frac{\hat{\tau}_c - \hat{\tau}_s}{T_s}\right) \times T_s \tag{11}$$
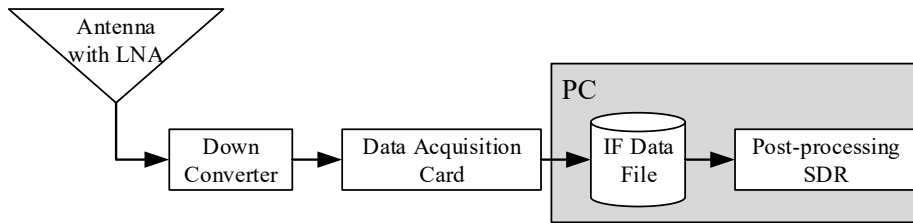
where $T_s = 1/2f_{sc,B1I}$ is the subcarrier chip width.

4. EXPERIMENTAL RESULTS

In order to verify the correctness and effectiveness of the proposed algorithm, some real experiments are done by using the live signals broadcast by BDS-3 satellites. First, the BDS-3 real-time software-defined receiver (SDR) [19] is modified as an intermediate-frequency (IF) signal recorder, which is used to acquire the zero-IF B1 wideband composite signal. Second, a post-processing SDR with the proposed method is developed to explore the ultra-high-performance ranging and positioning of the BDS B1 signal. More detailed, tracking results and positioning results are both given and analyzed. These results show that the subcarrier approximation is reasonable and the SCBOC modulated signal does contain ultra-high-performance ranging and positioning potential. In addition, the proposed method is verified to be able to fully exploit this potential.
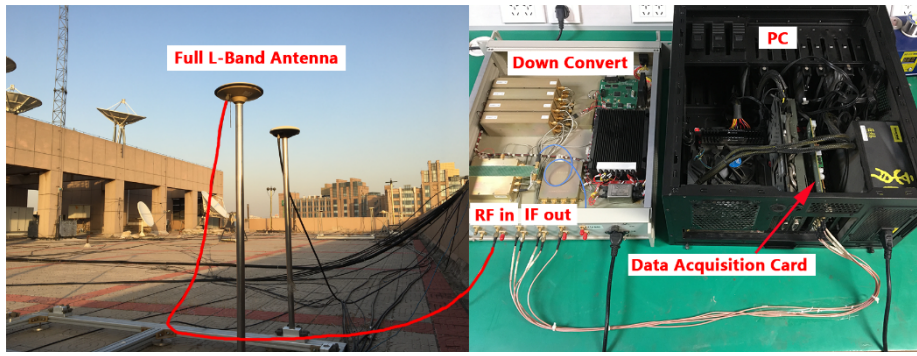
Experiment Setup

Figure 8 shows the schematic representation of the actual experiments. First, the full L-band antenna with a low noise amplifier (LNA) receives all RF signals from visible satellites in the horizon. Second, the front-end down-converts the received RF signals to the analog IF signals, which are then converted into digital baseband signals by the data acquisition card. Third, the zero-IF B1 wideband composite signal can be acquired and recorded as zero-IF data files in PC by the modified BDS-3 real-time SDR. Finally, a developed post-processing SDR with the proposed method is used to analysis these recorded signals.
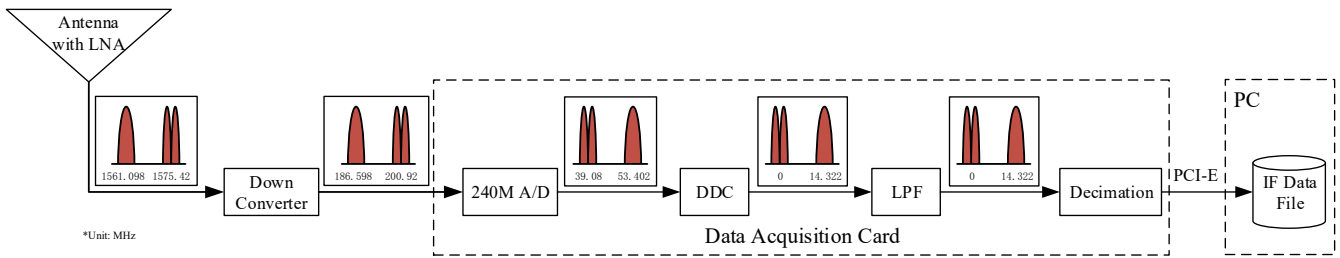

Figure 8: Schematic representation of the actual experiment

Figure 9 shows the working environment and equipment entity of the actual experiment. First, The full L-band antenna with LNA was laid on the roof of the Weiqing Building of Tsinghua University in Beijing where the latitude and longitude coordinates are 40.001461 and 116.330074, respectively. Second, the input frequency range of the down convert is from 1559 MHz to 1610 MHz, which means the B1 wideband composite signal can be received in the same channel. After the analog downconversion, the center frequency shifts from 1584.5 MHz down to 210 MHz. Third, the obtained analog IF signals are input into the analog-to-digital (A/D) converter of the data acquisition card to get digital IF signals. The bandpass sampling frequency at the A/D converter is 240 MHz. Then, the digital IF signals are sequentially processed by the digital downconversion (DDC), low-pass filter (LPF), and decimation to obtain the zero-IF signals with appropriate sampling rate. Next, these digital baseband signals are transmitted to the host PC through high-speed serial interface Peripheral Component Interconnect Express (PCI-E) and stored as zero-IF data files. Finally, these date files are processed and analyzed by the post-processing SDR on the PC.

Figure 9: Working environment and equipment entity

Figure 10 shows the detailed schematic diagram of spectrum during the acquisition of zero-IF signal data. It can be seen from Figure 10 that the spectrum of the B1 baseband composite signal acquired by our front-end is the mirror image of the theoretical spectrum. The reason is that the selected downconversion frequency and sampling rate in the design of our front-end. Note that the mirrored spectrum will not affect the ranging and positioning performance of the B1 composite signal. In addition, the mirrored spectrum also has little influence on the design and use of receiver. It should also be noted that the front-end bandwidth should be wide enough to contain the whole B1 wideband composite signal

during the acquisition of zero-IF signal data. The complex sampling is used in our design of the front-end and the complex sampling frequency is 20 MHz.

Figure 10: Schematic diagram of spectrum during the acquisition of zero-IF signal data
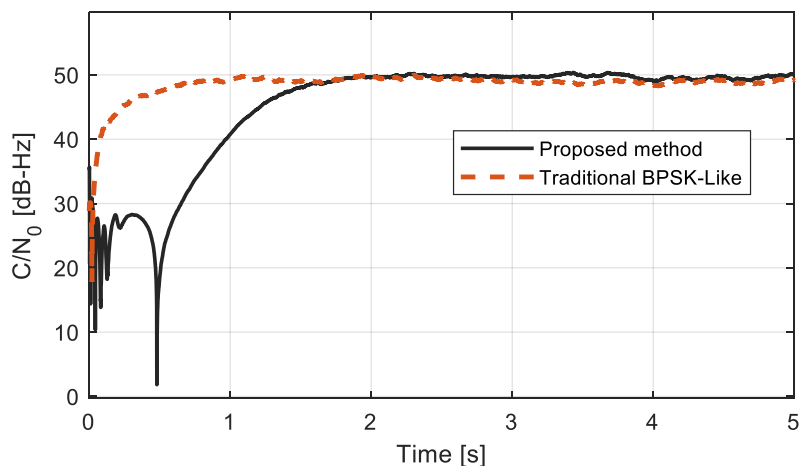
After acquiring the zero-IF signal data, a post-processing SDR with the proposed method is developed to explore the ultra-high-performance ranging and positioning of the BDS B1 wideband composite signal. More detailed, the tracking results of a single channel are given to show that our subcarrier approximation is reasonable and the proposed method can stably track the composite signal. In addition, the positioning results using multiple channels are also given to show that the SCBOC modulated signal does contain ultra-high-performance positioning potential and the proposed algorithm is verified to be able to fully exploit this potential.

Tracking Results

In this part, the tracking results of a single channel are given in three aspects, which are C/N_0 estimation results, correlator output results and correlation function curves.
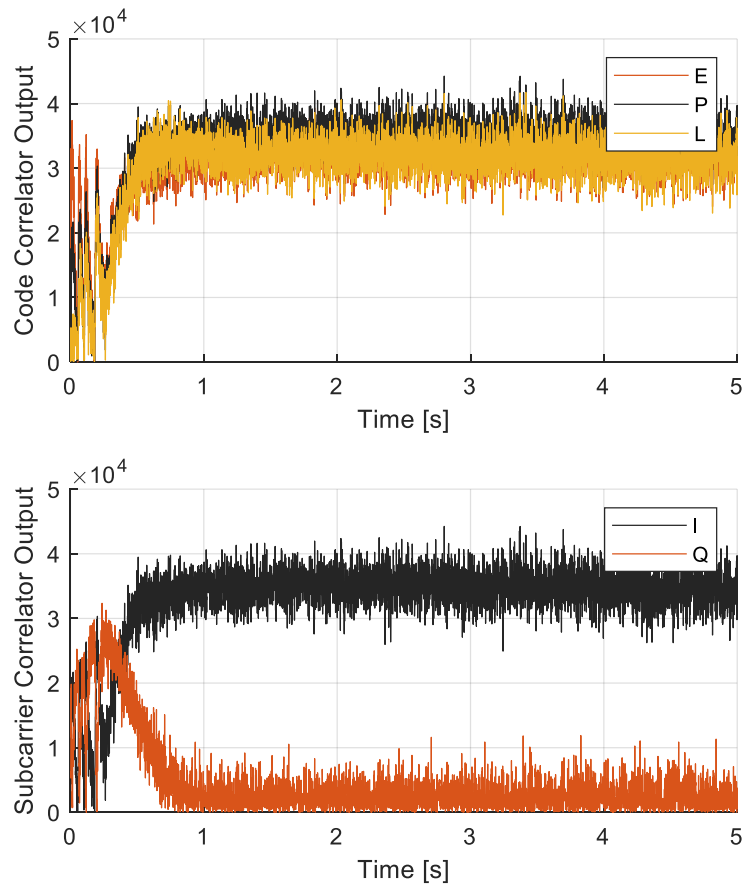
Figure 11 shows the C/N_0 estimation results of the proposed method for tracking the BDS-3 SCBOC modulated signal. As a comparison, the C/N_0 estimation results using the traditional BPSK-Like method for processing the BDS-3 B1I signal is also given. It can be seen from Figure 11 that after about 2 seconds, the C/N_0 estimation results of the proposed method tend to be stable, which means the proposed method can stably track the BDS-3 SCBOC(14,2) modulated signal. However, from the comparison of the C/N_0 estimation results between the proposed method and traditional BPSK-Like technique, it can be seen that the proposed method usually takes a longer time to enter the stable tracking phase. The reason for this difference is that the

traditional BPSK-Like method ignores the ranging capability brought by subcarrier component, while the proposed method wants to use it. Since the subcarrier of the SCBOC(14,2) modulated signal is approximated as pure sinusoid, there exists the complex coupling relationship between the carrier and the subcarrier. Therefore, the proposed method wants to use the subcarrier for ranging and positioning, then it needs first to complete the decoupling of the carrier and subcarrier, which means stable tracking of the carrier comes first and it takes some time. Although it needs more time in the initial tracking phase with the proposed method than the traditional BPSK-Like technique, the following results will show that it is worthwhile to spend these little costs.
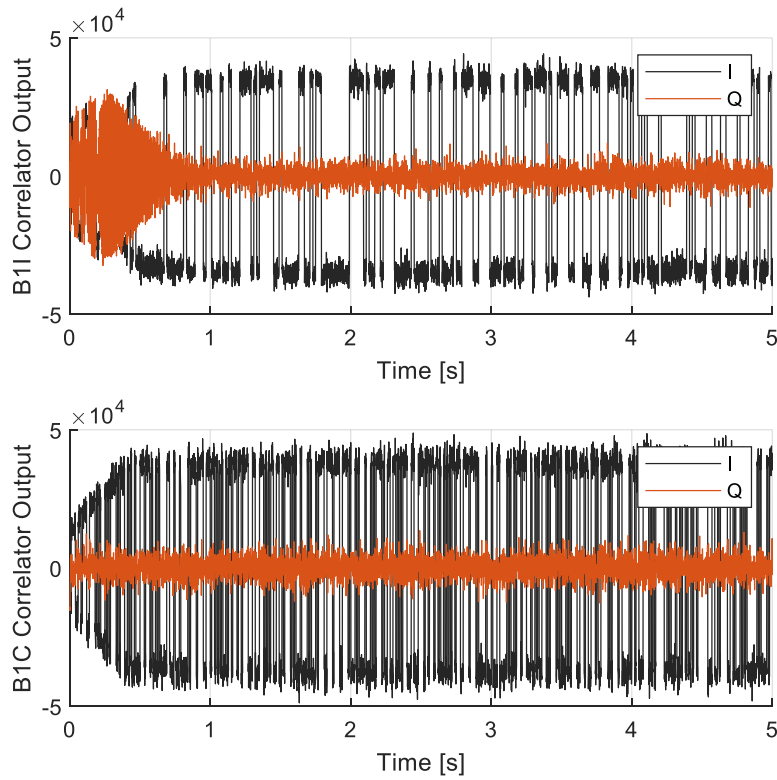

Figure 11: The comparison of the C/N_0 estimation results between the proposed method and the traditional BPSK-Like method

Figure 12 shows the absolute correlator outputs of the proposed tracking method in code dimension (up) and subcarrier dimension (down). As can be seen from the upper part of Figure 12, the prompt correlator has the largest absolute output among the early, prompt, and late correlators, which means the proposed method can stably track the SCBOC modulated signal in code dimension. Meanwhile, the lower part of Figure 12 shows that the in-phase (I) branch of the absolute correlator output in subcarrier dimension has much more power than quadrature (Q) branch, which means the subcarrier of the SCBOC modulated signal can be well tracked.
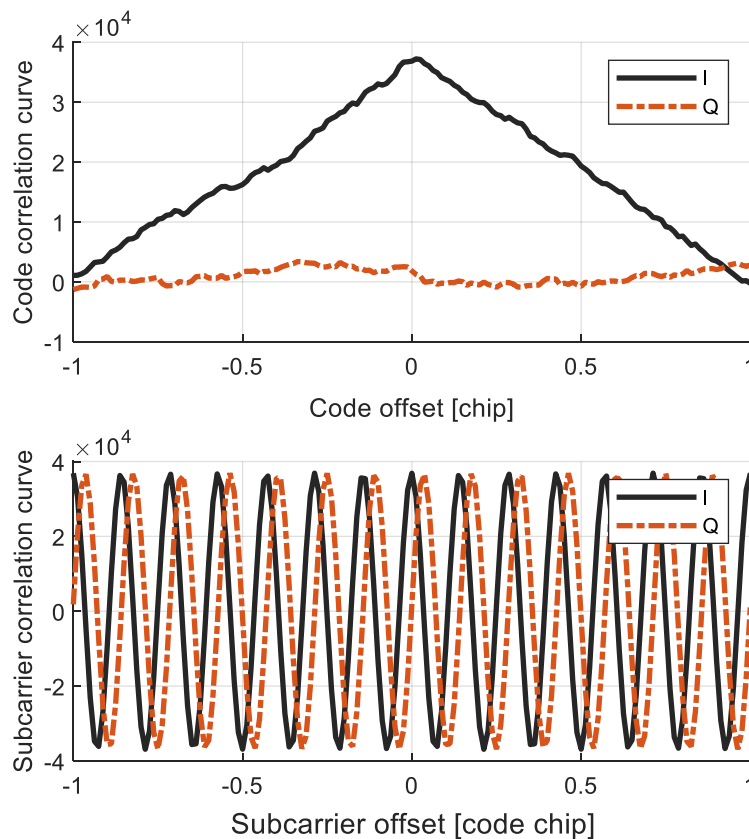
Figure 12: The absolute correlator outputs of the proposed method in code dimension (up) and subcarrier dimension (down)

Figure 13 shows the prompt correlator outputs of the BDS-3 B1I (Up) and B1C (down) signals with the proposed tracking method, including I and Q branches. It should be noted that the secondary code modulated on the B1I navigation message has been removed. As can be seen from the upper part of Figure 13, the correct B1I navigation bits are parsed in the I branch, which means the proposed tracking method can work well with the SCBOC modulated signal. In addition, the lower part of Figure 13 shows that the main power of prompt correlator outputs for B1C pilot channel is located at the I branch rather than the Q branch, which means the carrier of the BDS-3 B1 wideband composite signal has been perfectly tracked. Since the B1C pilot component is modulated with the overlay code, the bits' flow can be clearly seen in the I branch.

Figure 13: The prompt correlator outputs of the BDS-3 B1I (up) and B1C (down) signals with the proposed tracking method

Considering that there exist some drawbacks in the results of C/N_0 estimation and correlator output for directly deriving the correctness of the proposed tracking algorithm, the correlation function curves outlined by the multi-correlator technique are also given below.
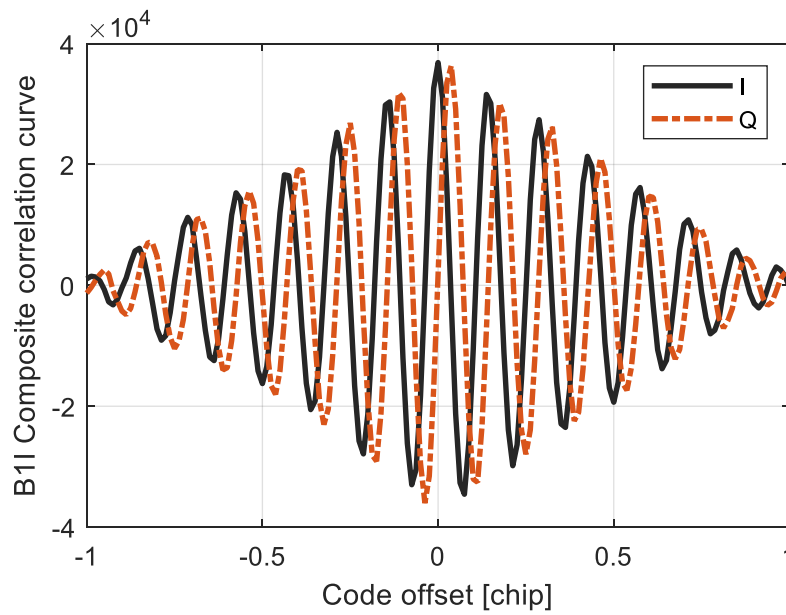
Figure 14 shows the correlation function curve of the SCBOC(14,2) modulated signal with proposed tracking method in code dimension (up) and subcarrier dimension (down) using multiple-correlator technique. As can be seen from the upper part of Figure 14, the correlation function curve in code dimension is a standard correlation function shape of the BPSK(2) modulated signal, which means the ranging code can be perfectly recovered. In addition, the lower part of Figure 14 shows that the correlation function curve in the subcarrier dimension is like a periodic sinusoid instead of a sawtooth wave, which means the original peaks are smoothed due to the influence of front-end bandlimiting filter. Therefore, the subcarrier approximation in signal model is reasonable. In addition, as can be seen from the lower part of Figure 14, when the locally replicated subcarriers are aligned with the subcarriers in the received signal, that is subcarrier offset equals 0, the main power of the subcarrier correlation function is located in the I branch and the power in Q branch is approximated as 0, which means the complex subcarrier of the SCBOC modulated signal can be well tracked by the proposed method.

Figure 14: The correlation function curve of the SCBOC(14,2) modulated signal with proposed tracking method in code dimension (up) and subcarrier dimension (down)

Figure 15 shows the correlation function curve of the SCBOC(14,2) modulated signal with proposed tracking method in composite dimension using multiple correlator technique. Compared with the ideal ACF of the SCBOC(14,2) modulated signal in Figure 6, it can be seen that the correlation function curve matches well with the ideal ACF except for the smoothed peaks and mirrored Q branch. As mentioned before, the smoothed peaks in the correlation function curve are due to the influence of the front-end bandlimiting filter on the complex subcarrier. As for the mirrored relationship of the Q branch between the correlation function curve and the ideal ACF, this is due to the acquired zero-IF signal data has the mirrored spectrum as shown in Figure 10. Apart from these differences, the correlation function curve matches well with the ideal ACF, which means the proposed method can achieve the high-precision unambiguous tracking of the SCBOC(14,2) modulated signal. More specifically, the prompt tracking point, which corresponds to the position of 0 code offset in the correlation function curve, locates at the main peak rather than other side peaks, which means the tracking ambiguities threat has been overcome. In addition, the main energy of the prompt tracking point is maintained in the I branch rather than the Q branch, which means the complex coupling relationship between the carrier and the subcarrier has also been decoupled. These results clearly reveal the correctness of the proposed tracking algorithm.

Figure 15: The correlation function curve of the SCBOC(14,2) modulated signal with proposed tracking method in composite dimension

Figure 16 shows the correlation function curve of the B1C pilot BOC(1,1) component with proposed tracking method using multiple correlator technique. First, as can be seen from Figure 16, the correlation function curve is a standard correlation function shape of the BOC(1,1) modulated signal, which means the ranging code and subcarrier of B1C pilot BOC(1,1) component can be perfectly recovered. Second, compared with Figure 14, the correlation results of the B1C pilot BOC(1,1) component with the proposed tracking method will not ever fall into the gray area in Figure 16, which means tracking on the side peaks instead of the main peak for B1C signal will not occur. This is because the ranging code of the B1I signal is used to generate the locally replicated ranging code and subcarrier of B1C pilot BOC(1,1) component in the proposed method. Therefore, the ambiguity threat of the B1C pilot BOC(1,1) component was cleverly erased and the receiver robustness is also improved.
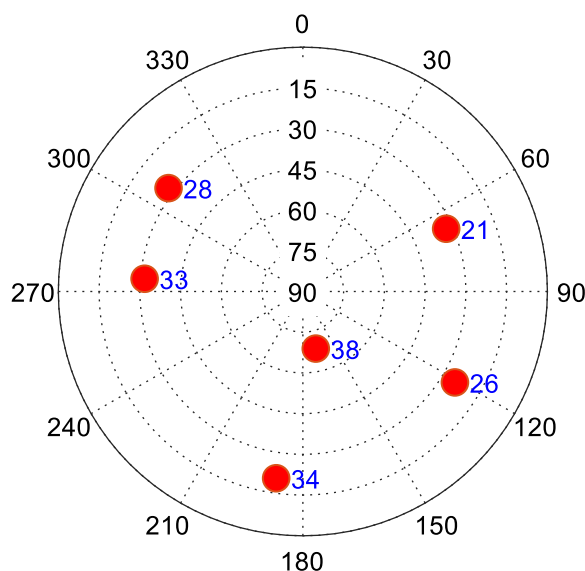

Figure 16: The correlation function curve of the B1C pilot BOC(1,1) component with proposed tracking method

The tracking results above of a single channel show that the subcarrier approximation in the signal model is reasonable and the proposed method can stably and correctly track the BDS B1 wideband composite signal. In order to have more understanding of the proposed method, the positioning results using multiple channels are also given below.
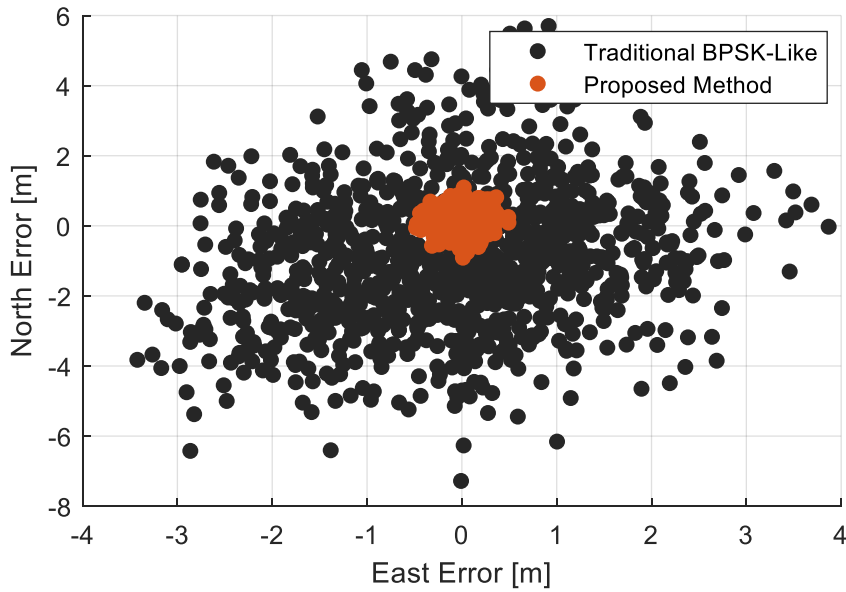
Positioning Results

In this part, the positioning results using multiple channels are given and analyzed to verify that the SCBOC(14,2) modulated signal does contain ultra-high-performance positioning potential and the proposed algorithm can fully exploit this potential.

Figure 17 shows the skyplot of BDS-3 satellites at Tsinghua University at 04:32 (BDST) on October 29, 2019. As can be seen from Figure 17, there are 6 available satellites in the sky and their prn numbers are 21, 26, 28, 33, 34, 38, respectively. The position dilution of precision (PDOP) value is 2.24, which is good enough to complete stable single-point positioning. It is not difficult to predict that with the construction of the BDS-3, the number of available BDS-3 satellites will increase and the distribution of BDS-3 satellites will improve. Therefore, the positioning precision will be higher than now.

Figure 17: The skyplot of BDS-3 satellites at Tsinghua University at 04:32 (BDST) on October 29, 2019

Figure 18 shows the horizontal positioning errors of SCBOC(14,2) modulated signal with the proposed tracking method. As a comparison, the horizontal positioning errors of BDS-3 B1I signal using the traditional BPSK-Like technique are also given. It can be clearly seen from Figure 18 that the proposed tracking method has a significant improvement in positioning precision due to the full utilization of the high-frequency subcarrier ranging performance. More specifically, compared with the traditional BPSK-like reception technique, the proposed method reduces the east error from about ±4 m to ±0.5 m, and the north error is reduced from around ±6 m to ±1 m. Therefore, the proposed tracking method is expected to be utilized in the sub-meter positioning applications.

Figure 18: The comparison of the horizontal positioning errors between the proposed tracking method and the traditional BPSK-Like technique

The positioning results above show that the BDS-3 SCBOC(14,2) modulated signal does contain ultra-high-performance positioning potential and that the proposed tracking algorithm is able to fully exploit this potential. These new significant understanding and results can provide great guidance and reference for BDS receiver designers.

5. CONCLUSION

In order to achieve backward compatibility and multi-frequency multiplexing, a unique SCBOC(14,2) modulation type was introduced in the BDS-3 B1 composite signal. This paper first points out that the BDS-3 SCBOC(14,2) modulated signal may also contain the ultra-high-precision ranging potential except for being a transparent multiplexing component, and then proposes an example solution to verify that this potential can be utilized. The work and contribution of this paper are mainly reflected in two aspects.

First, the ranging possibility and tracking challenges of the new SCBOC(14,2) modulated signal are proposed and analyzed. Starting from the generation background and signal model, the characteristics of the SCBOC(14,2) modulated signal are studied in detail, including the PSD, Gabor bandwidth, and ACF. The results of the Gabor bandwidth show that the SCBOC(14,2) modulated signal may contain ultra-high-precision ranging potential, which deserves the attention and research of receiver designers. However, the results of the ACF show that there exist two main tracking challenges for processing the SCBOC(14,2) modulated signal. One problem is the famous tracking ambiguity threat inherent in BOC-class modulated signals. And the other one is the existence of the complicated coupling relationship between the subcarrier and carrier in the correlation function. These challenges hinder the understanding and utilization of SCBOC modulated signals.

Second, an unambiguous tracking method is proposed to be an example solution to explore the ultra-high-precision ranging potential of the BDS B1 signal. More detailed, it uses a 2-dimensional loop structure to address the ambiguity threat inherent in BOC-class modulated signals. In addition, based on the coherence between the components of the composite signal, the proposed method uses cross-assisted technique to solve the coupling problem in the correlation function between subcarrier and carrier while improving the receiver robustness. Real experimental results using live BDS-3 signals verified the correctness and effectiveness of the proposed algorithm.

For BDS receiver designers who are interested in the high-precision ranging, this paper can provide great guidance and reference. As for future research, other unambiguous tracking methods for BDS-3 B1 signal are recommended. In addition, the influence of the ionosphere on the BDS-3 B1 wideband composite signal is also worthy of attention.

ACKNOWLEDGMENTS

REFERENCES

1.   Yao Z, Lu M. Constant envelope combination for components on different carrier frequencies with unequal power allocation. Proceedings of the ION ITM. 2013:629-37.

2.   Yao Z, Guo F, Ma J, Lu M. Orthogonality-based generalized multicarrier constant envelope multiplexing for DSSS signals. IEEE Transactions on Aerospace and Electronic Systems. 2017;53(4):1685-98.

3.   Yao Z, Lu M. Signal multiplexing techniques for GNSS: the principle, progress, and challenges within a uniform framework. IEEE Signal Processing Magazine. 2017;34(5):16-26.

4.   Sleewaegen J-M, De Wilde W, Hollreiser M, editors. Galileo ALTBOC receiver. Proceedings of GNSS; 2004.

5.   Hodgart M, Blunt P, Unwin M, editors. The optimal dual estimate solution for robust tracking of binary offset carrier (BOC) modulation. Proceeding of ION GNSS; 2007.

6.   Borio D. Double phase estimator: new unambiguous binary offset carrier tracking algorithm. IET Radar, Sonar & Navigation. 2014;8(7):729-41.

7.   Borio D. Coherent side-band BOC processing. IET Radar, Sonar & Navigation. 2017;11(10):1455-66.

8.   Feng T, Kai Z, Liang C. Unambiguous tracking of BOC signals using coherent combination of dual sidebands. IEEE Communications Letters. 2016;20(8):1555-8.

9.   Schubert FM, Wendel J, Soellner M, Kaindl M, Kohl R, Ieee. The Astrium Correlator: Unambiguous Tracking of High-Rate BOC Signals.   2014 Ieee/Ion Position, Location and Navigation Symposium - Plans 2014. IEEE-ION Position Location and Navigation Symposium2014. p. 589-601.

10.   Lohan ES, de Diego DA, Lopez-Salcedo JA, Seco-Granados G, Boto P, Fernandes P. Unambiguous techniques modernized GNSS signals: surveying the solutions. IEEE Signal Processing Magazine. 2017;34(5):38-52.

11.   Yao Z, Gao Y, Gao Y, Lu M. Generalized Theory of BOC Signal Unambiguous Tracking with Two-Dimensional Loops. IEEE Transactions on Aerospace and Electronic Systems. 2017;53(6):3056-69.

12.   Gao Y, Yao Z, Lu M. Theoretical analysis of unambiguous 2-D tracking loop performance for band-limited BOC signals. GPS Solutions. 2018;22(1):30.

13.   Martin N, Leblond V, Guillotel G, Heiries V, editors. BOC (x, y) signal acquisition techniques and performances. Proceedings of the 16th International Technical Meeting of the Satellite Division of The Institute of Navigation (ION GPS/GNSS 2003); 2001.

14.   AVILA-RODRIGUEZ JA, Hein GW, Wallner S, ISSLER JL, Ries L, Lestarquit L, et al. The MBOC modulation: the final touch to the Galileo frequency and signal plan. Navigation. 2008;55(1):15-28.

15.   Hein GW, Avila-Rodriguez J-A, Wallner S, Pratt AR, Owen J, Issler J-L, et al. MBOC: the new optimized spreading modulation recommended for GALILEO L1 OS and GPS L1C. Proceedings of IEEE/ION PLANS. 2006;2006:884-92.

16.   Yao Z, Lu M, Feng Z. Quadrature multiplexed BOC modulation for interoperable GNSS signals. Electronics letters. 2010;46(17):1234-6.

17.   Lestarquit L, Artaud G, Issler J-L, editors. AltBOC for dummies or everything you always wanted to know about AltBOC.

ION GNSS; 2008.

18.   Gao Y, Yao Z, Lu M. High-precision unambiguous tracking technique for BDS B1 wideband composite signal. Navigation. 2020.

19.   Gao Y, Yao Z, Lu M. Design and implementation of a real-time software receiver for BDS-3 signals. Navigation. 2019;66(1):83-97.